Supplementary Information

3D optical Yagi-Uda nanoantenna-array

DANIEL DREGELY, RICHARD TAUBERT, JENS DORFMÜLLER, RALF VOGELGESANG, KLAUS KERN, AND HARALD GIESSEN

Supplementary Figures

a

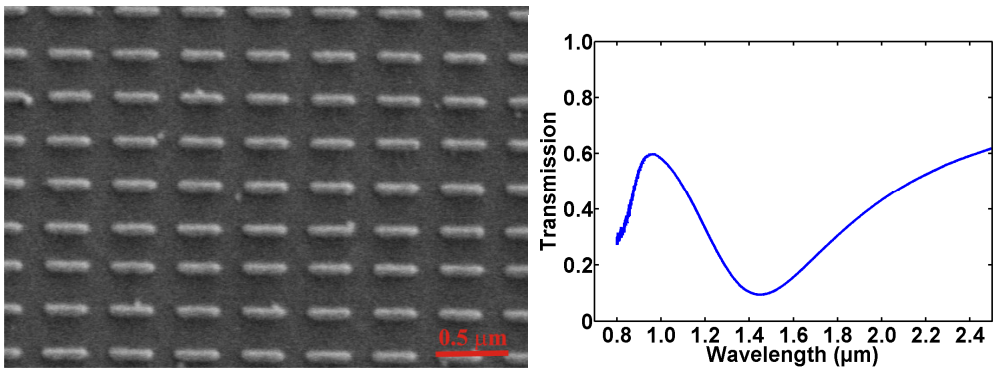

b

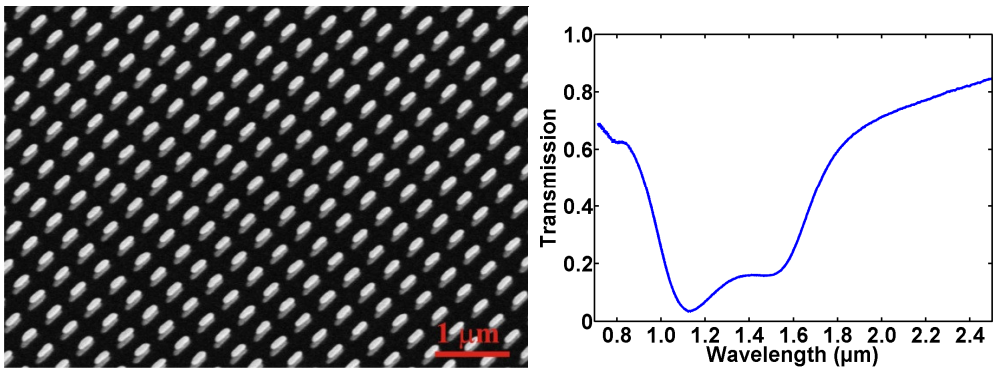

c

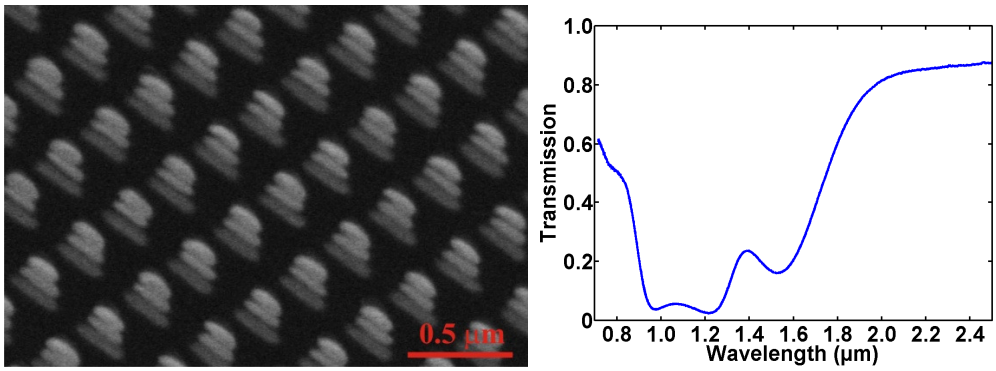

Supplementary Figure S1 | Coupling between the layers. The nearfield coupling between the layers can be observed as a spectral hybridization of the plasmonic resonances. The left column shows SEM-pictures of the a) one layer, b) two layer and c) three layer structure. The right column shows the according transmission spectra of the array structure.

a

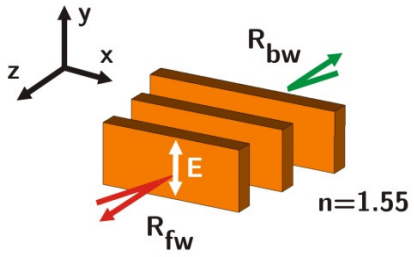

b

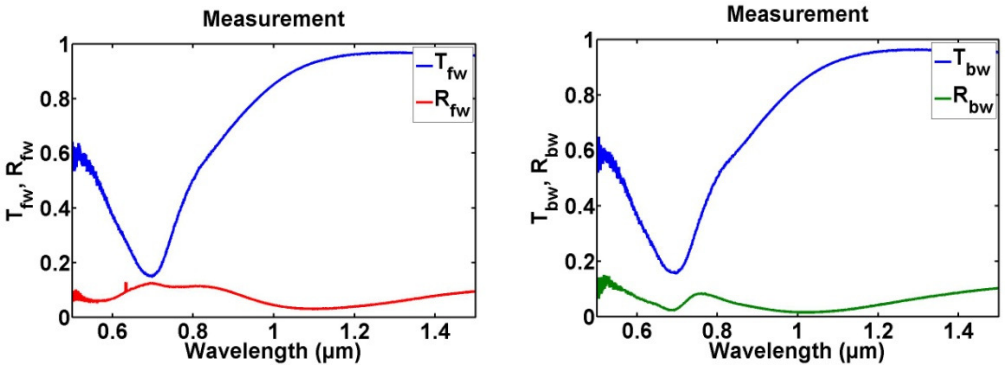

Supplementary Figure S2 | Polarization perpendicular to the rod-axes. a) Polarization of the incident electric field along the y-direction. b) Left plot shows transmission and reflection spectra for forward incidence and right plot for backward incidence. Compared to Fig. 3, the significant difference between forward and backward direction in the spectra disappear when the polarization of the incident electric field is set along the y-direction. This proves that the directionality of the antenna is an effect that is tied to its Yagi-Uda properties, which are only present for polarization along the x-direction.

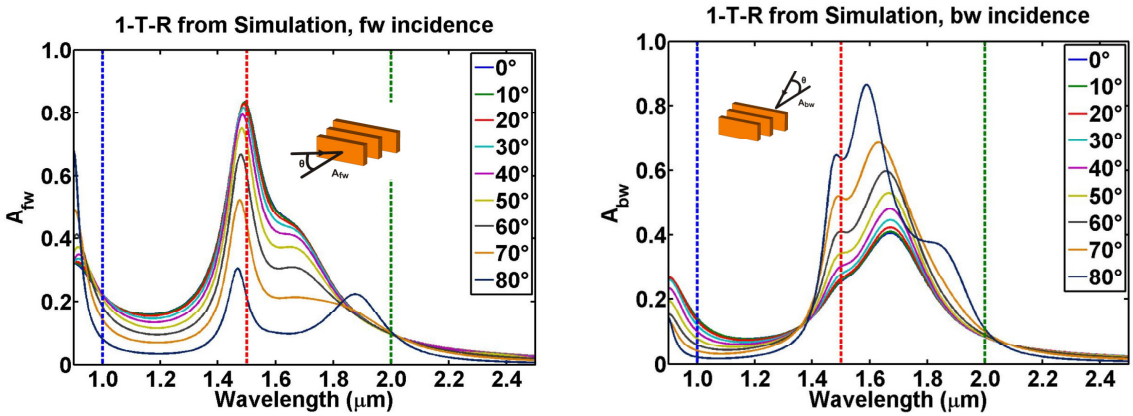

Supplementary Figure S3 | Angle dependence of absorption spectra. We simulated the reflection and transmission spectra for different angles of incidence and calculate the angle dependent absorption spectra (A = 1-T-R) for forward (left plot) and backward (right plot) incidence. The significant difference for different incident angles comes mainly from the reflection coefficients (not shown) that show a strong dependency on the incident angle. For transmission no significant difference occurs at different incident angles (not shown). This is in agreement with angle dependent transmission experiments carried out up to an angle of 30° (not shown). The dashed lines indicate the spectral position of the absorption coefficients plotted in Supplementary Figure S4.

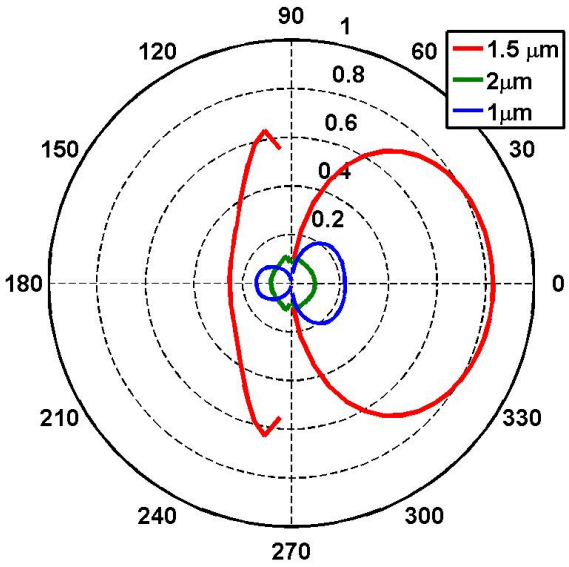

Supplementary Figure S4 | Extracted absorption radiation pattern. Polar plot of the absorption coefficients as function of angle of incident radiation at the particular spectral positions of Fig. S3.

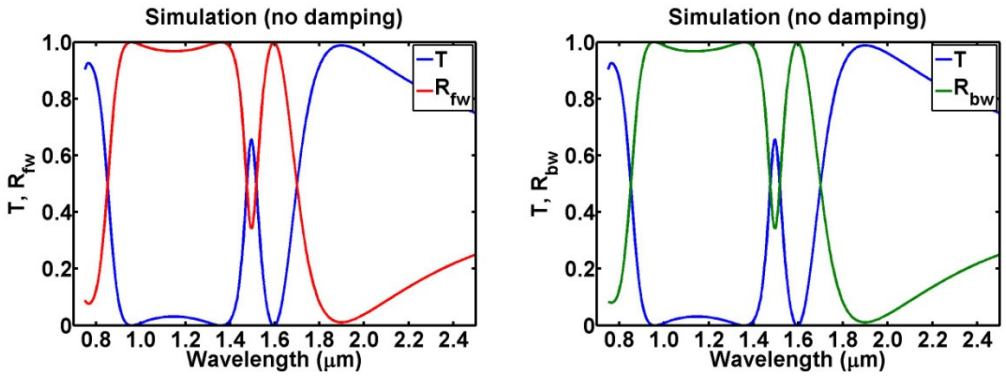

Supplementary Figure S5 | No damping. Transmission and reflection spectra for the no damping case (Drude damping set to zero in the simulations). The left plot shows the spectra for forward incidence and the right plot for backward incidence. The forward and backward reflection of the antenna array is symmetric when no energy dissipation in the gold rods takes place.

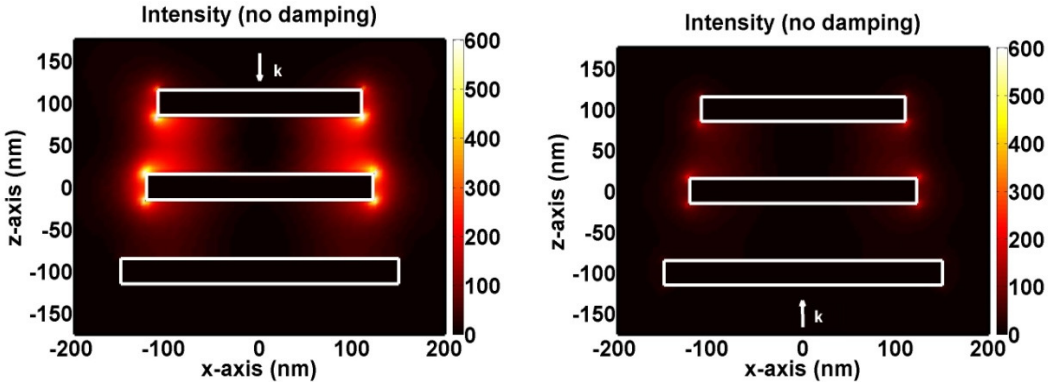

Supplementary Figure S6 | Numerically calculated nearfield intensity with turned off damping. The structure is illuminated from the forward direction in the left plot and from the backward direction in the right plot. The near field still is confined to the tips of the feed element when the array is illuminated from the forward direction.

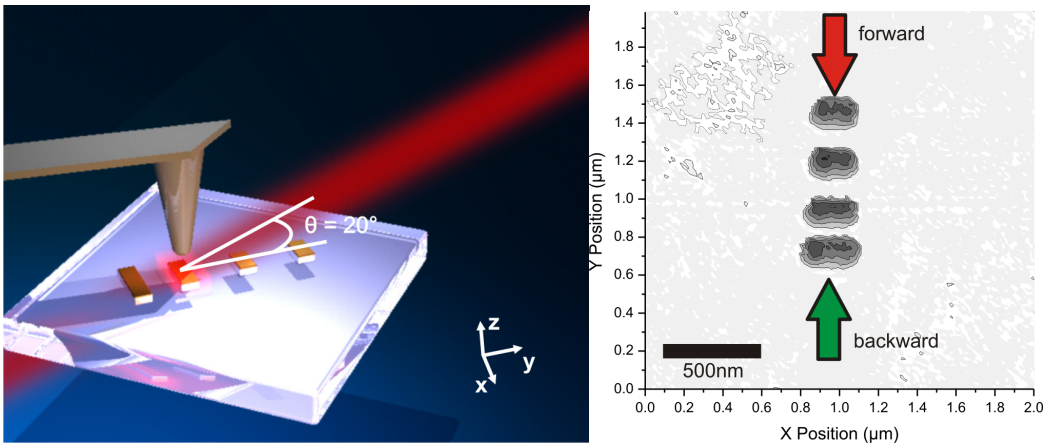

Supplementary Figure S7 | Nearfield measurements on a planar Yagi-Uda antenna. We confirm the concentration of fields at the feed element of an optical Yagi-Uda antenna in receiving mode experimentally by measuring the electric nearfield for a 2D planar Yagi-Uda antenna on a glass substrate. For the planar antenna the upper half space is not covered and we can access the nearfield with an apertureless Scanning Nearfield Optical Microscope (aSNOM)[22, 27] probe. Left panel: Schematic of the measurement setup. The incident light (at the antenna's resonant wavelength λ = 1064 nm) is polarized along the x-axis and excites the structure at an angle of 20° with respect to the antenna plane. Right panel: Topographic image of the planar Yagi-Uda nanoantenna.

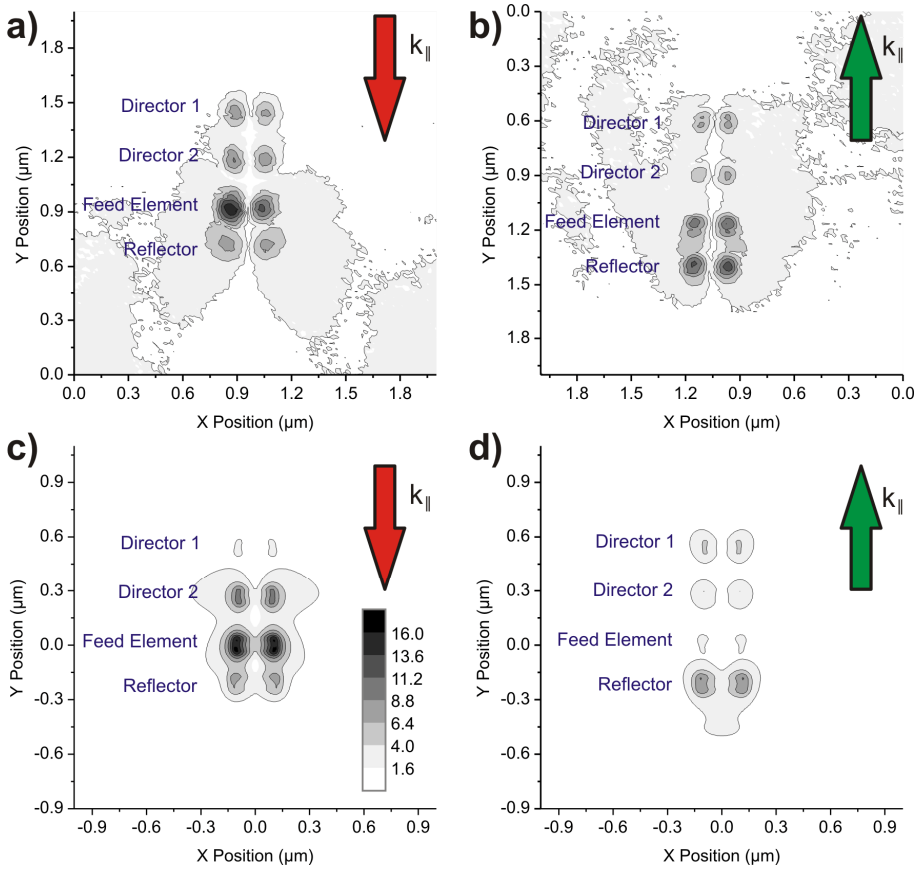

Supplementary Figure S8 | Comparison between measured and simulated electric nearfield amplitude. a) The aSNOM image for forward incident light shows an enhanced nearfield (E_z-component) at the tips of the feed element. Clearly, only the feed element lights up whereas b) for backward incidence the energy is more evenly distributed over all elements. In order to compare the electric field amplitudes, we simulate the nearfield enhancement for the experimental configuration and extract the amplitude of the E_z-component c) for forward and d) for backward incidence. Simulation and experiment are very consistent. The maximum field is at the tips of the feed element for forward incident light. Additionally, the nearfield simulations show that the overall nearfield amplitude for backward incident light is lower. Since the 3D Yagi-Uda antenna is completely embedded in a dielectric environment, its nearfield distribution under excitation is not measurable. However, the correspondence of Figure 4b (left) to Figure S8 c), which is consistent with the experiments on the 2D structure, strongly supports the interpretation of field confinement to the feed element, also in the 3D case. The scale bar is normalized to the field strength of the incoming light.

Supplementary References

27. Bek, A. et al. Aperture less scanning near field optical microscope with sub-10 nm resolution. *Rev. Sci. Instrum.* **77**, 043703 (2006).